A Ray-tracing simulation of High Frequency radio wave propagation in Antarctica during the December 4, 2021 total solar eclipse

Binjie Liu[1], Gareth Perry[1], Joe Huba[2], Lindsay Goodwin[1,3] and William Bristow[4]

1. Center for Solar-Terrestrial Research, New Jersey Institute of Technology
2. Syntek Technologies
3. University Corporation of Atmospheric Research
4. Penn State

INTRODUCTION

- High Frequency (HF) radio waves are highly sensitive to plasma density variations in the ionosphere.
- A solar eclipse causes a significant reduction of the plasma temperature and plasma density, leading to a change in HF radio wave propagation conditions (refractive index) in the ionosphere.
- Ionospheric irregularities impact high frequency (HF; 3—30 MHz) radio waves, which can have a negative influence on telecommunications (Weber et al., 1984).
- This work presents a raytracing simulation of the Doppler shift of McMurdo SuperDARN transmissions received by the Radio Receiver Instrument (RRI) onboard the e-POP during the December 4 eclipse using PHaRLAP based on the ionospheric plasma density generated by the SAMI3 model.

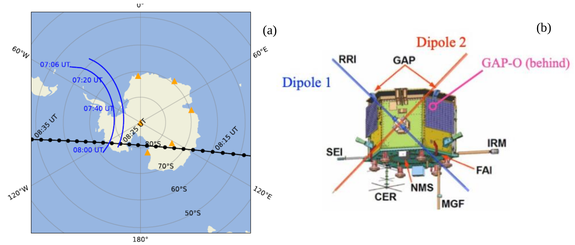

Figure 1 (a) The map above shows the e-POP trajectory (black) and the eclipse path (width of umbra's path in blue). (b) e-POP diagram (Perry et al., 2017) focusing on two of those instruments: RRI and Global Position System receiver-based Attitude, Position, and profiling experiment – Occultation(*GAP-O).*

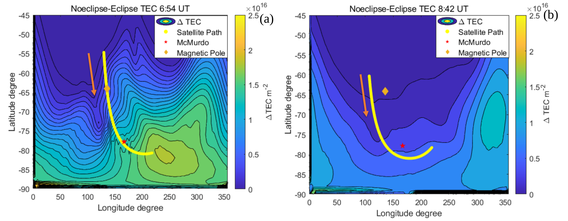

Figure 2 Spacecraft trajectory (yellow trace) with background as TEC difference between Eclipse and No Eclipse case. The high TEC area represents the eclipse. The orange arrow shows the direction of the spacecraft. The TEC values are derived from a SAMI3 simulation.

- ΔTEC is the TEC of No eclipse subtract the TEC of Eclipse.
- The maximum of ΔTEC is approximately 1.8 TECU.

OBJECTIVE

Use HF ray-trace modeling based on the ionospheric information from SAMI3 to simulate the Doppler shift of 10.3 MHz rays transmitted from McMurdo received by e-POP for eclipse and no eclipse case. By doing so, we will be able to gain insight into the impact of the eclipse on the earth's ionosphere.

METHODOLOGY

- Ray-tracing package: PHaRLAP (Cervera et al., 2014).
- Ionosphere: SAMI3 (Huba et al., 2020).
- Magnetic field: IGRF 2016 model.
- Date: December 4, 2021.
- Elevation angle: 3-81° increment of 0.2° .
- Bearing angle: 0-360 ° increment of 0.2°
- Frequencies： 10.3 MHz.
- Transmitter location: McMurdo Station (77° 50′ 47″ S 166° 40′ 06″ E)
- Receiver: e-POP spacecraft set receiving zone as 5 km sphere centered at spacecraft in real time.
- Spacecraft trajectory No. 1: 6:54:15 UT to 7:4:12 UT time increment 1 s.
- Spacecraft trajectory No. 2: 8:36:15 UT to 8:46:12 UT time increment 1 s.

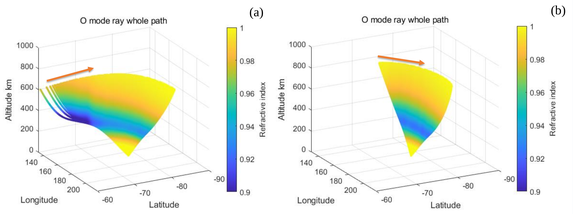

Figure 3 An example of 3D ray-tracing of all O mode rays received by the spacecraft during trajectory No. 1 (left) and trajectory No. 2 (right) under eclipse condition. Color coded with the refractive index along the ray. Orange arrow represents the direction that the spacecraft flew.

- Electron density in the ionosphere affect the refractive index of HF rays propagating through.
- Doppler shift of the rays received by the space craft :

$$\boldsymbol{\Delta\omega_{AB} = -k_0\left[\int_A^{B(t)} \frac{\partial n}{\partial t} ds + \frac{\partial B(t)}{\partial t} n(B)\right]} \qquad \textbf{(1)}$$

- $\Delta\omega_{AB}$ is the Doppler shift in angular frequency. k_0 is the wave vector of radio wave, B is the position of the receiver, A is the position of transmitter, n is the refractive index along the ray path.
- In the simulation, the time resolution of ionosphere is 6 minutes, and of the order of the spacecraft's measurement experiment.
- We assume that during the 6 minutes interval the ionosphere is fixed and the rays will scan through the ionosphere with the movement of the spacecraft.
- Simplify the equation and change the Doppler shift expression into frequency in Hz.

$$\boldsymbol{\Delta f = -\frac{1}{\lambda_0}\left[\frac{\partial}{\partial t}\int_A^{B(t)} n ds + \frac{\partial B(t)}{\partial t} n(B)\right]} \qquad \textbf{(2)}$$

- λ_0 is the wavelength of 10.3 MHz in meters.
- First term: the effect of refractive index change along the ray path. The integral is the phase path of the received ray.
- Second term: spacecraft velocity vector projected to the direction of wave vector at the receiving point.

SIMULATION RESULTS

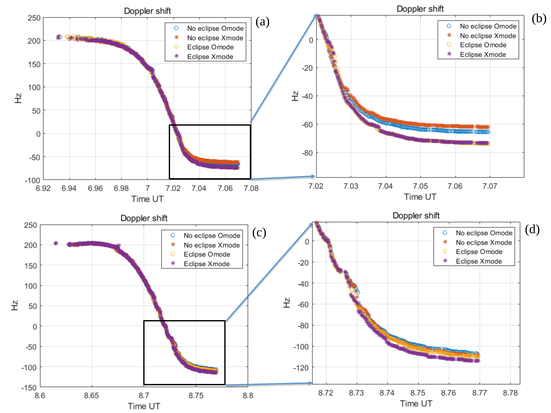

Figure 4 Doppler shift of the rays received by the spacecraft in Hz. Including the O and X modes under eclipse and no eclipse cases for spacecraft trajectory No. 1 (a),(b) and trajectory No. 2 (c), (d). Figure (b) and (d) are the zoomed in of the corresponding rectangular area highlighted in (a) and (c).

- In both trajectories at Doppler shift greater than zero (shortest distance between McMurdo and the e-POP) all four cases O and X mode under eclipse and non-eclipse case show that there is no significant difference in Doppler shift.
- After the shortest distance point both trajectories show deviation in Doppler shift frequency. The deviation increases as the spacecraft goes farther away from McMurdo.
- Trajectory No.1 maximum difference between eclipse and non-eclipse is 11.4 Hz in X mode. Trajectory No.2 maximum difference is 6.3 Hz in X mode.

DISCUSSION

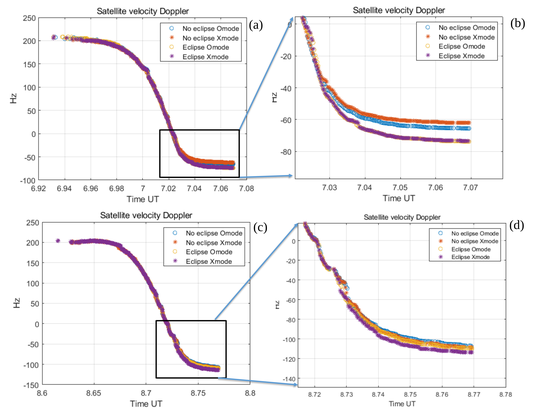

Figure 5 Doppler shift caused by the satellite velocity, the second term in Doppler equation 2. All four subfigures form with the same strategy as Figure 4.

DISCUSSION

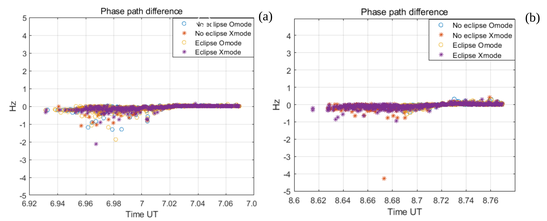

Figure 6 Doppler shift caused by the refractive index change along the ray path (first term in Doppler equation 2). (a) Doppler shift for trajectory No.1 (b) Doppler shift for trajectory No.2.

- The total Doppler shift curve is dominated by the angle between the wave vector k at the point ray reaches the receiving zone, and the spacecraft velocity.
- The Doppler shift caused by the phase path difference is the minor factor of the total Doppler shift. The maximum in trajectory No. 1 is -2.1 Hz and in trajectory No. 2 is -4.2 Hz.
- In trajectory No 1. the spacecraft experience more gradient of the ΔTEC and goes into the eclipse umbra while the trajectory No. 2 the eclipse umbra does not have that strong impact with the spacecraft after the spacecraft cross the shortest distance point from McMurdo.
- The time increment of the spacecraft location is 1 second, which means that the ray path experiences very similar ionosphere with its closest neighbor. Thus, the Doppler shift caused by phase path difference is very small, which is shown in Figure 6.

CONCLUSION AND FUTURE WORK

- Simulation results shows that during the eclipse, electron density in the ionosphere descent in an obvious amount (maximum 1.8 TECU).
- Doppler shift of HF radio wave is an effective tool to pick up the electron density change caused by eclipse.
- Simulation shows that the angle between wave vector and the spacecraft velocity at the receiving point is the dominant factor in Doppler shift.
- HF radio wave propagation is sensitive to electron density variation in the ionosphere.
- Future work will involve the experimental measurement data from RRI and compare that with the simulation results.

REFERENCES

Cervera, M. A., & Harris, T. J. (2014). Modeling ionospheric disturbance features in quasi-vertically incident ionograms using 3-D magnetoionic ray tracing and atmospheric gravity waves. Journal of Geophysical Research: Space Physics, 119(1), 431-440.

Weber, E. J., Buchau, J., Moore, J. G., Sharber, J. R., Livingston, R. C., Winningham, J. D., & Reinisch, B. W.(1984). F layer ionization patches in the polar cap. Journal of Geophysical Research: Space Physics, 89(A3), 1683-1694.

Perry, G. W., James, H. G., Gillies, R. G., Howarth, A., Hussey, G. C., McWilliams, K. A., Yau, A. W. (2017). First results of HF radio science with e-POP RRI and SuperDARN. *Radio Science*, *52*(1), 78–93. https://doi.org/10.1002/2016RS006142

Ponomarenko, P. V., St-Maurice, J. P., Waters, C. L., Gillies, R. G., & Koustov, A. V. (2009, November). Refractive index effects on the scatter volume location and Doppler velocity estimates of ionospheric HF backscatter echoes. In Annales Geophysicae (Vol. 27, No. 11, pp. 4207-4219). Copernicus GmbH.

Huba, J. D., & Liu, H. L. (2020). Global modeling of equatorial spread F with SAMI3/WACCM-X. *Geophysical Research Letters*, *47*(14), e2020GL088258.

RESEARCH POSTER PRESENTATION DESIGN © 2018
www.PosterPresentations.com